Dynamic Crystallization of Polypropylene and Wood-Based Composites

R. Bouza,[1] C. Marco,[2] Z. Martín,[2] M. A. Gómez,[2] G. Ellis,[2] L. Barral[1]*

[1]*Department of Physics, E.U.P. Ferrol, Universidad de A Coruña, 15405 Ferrol, Spain*
[2]*Instituto de Ciencia y Tecnología de Polímeros, CSIC, 28006 Madrid, Spain*

Received 9 May 2006; accepted 13 July 2006
DOI 10.1002/app.25211
Published online in Wiley InterScience (www.interscience.wiley.com).

ABSTRACT: Thermoplastic composites made of an isotactic polypropylene (iPP) matrix and woodflour (WF) were prepared by melt-blending, using twin-screw extrusion and injection molding. Up to 20 wt % of the composite was composed of WF. The incorporation of an interfacial agent made of an ethylene/methacrylic acid copolymer to iPP and WF, PP/WF, binary blends causes a compatibilization effect that becomes evident due to a reduction in the crystallization temperature of PP. In both the binary composites and the compatibilized or ternary composites, the PP adopts an α or monoclinic structure when crystallization occurs from the melt under dynamic conditions at cooling rates between 1 and 20°C min^{-1}. On the other hand, X-ray diffraction analysis using synchrotron radiation of the injection-molded samples demonstrates the existence of a β or trigonal form in the binary as well as the ternary PP/WF composites. They reach k_β levels between 0.18 and 0.25, which can be interpreted as the co-operation between a reduction of the crystallization rate and the shear effect induced during the injection. © 2006 Wiley Periodicals, Inc. J Appl Polym Sci 102: 6028–6036, 2006

Key words: polymer blends; woodflour/polypropylene; differential scanning calorimetry; crystallization; β-phase

INTRODUCTION

Over the last few years, a considerable growth in the consumption of polymeric composites reinforced with fibers has taken place, thus allowing the development of a wide range of composites as alternatives to conventional materials like metal and wood.[1] These composite materials have a unique combination of high performance, great versatility, processing advantages, and reasonable costs.[2]

Inorganic reinforcements currently dominate ~ 90% of the reinforced thermoplastics industry, while natural fibers make up the remaining 10%. The substitution of inorganic reinforcements with other natural ones, like vegetable fibers, has many advantages. One of the most important advantages is less pollution due to the biodegradability of fibers and combustibility, which does not cause the production of toxic gases or solid wastes. Simple particles or fibers or bundles of fibers can be used, since they have lower density and excellent deformation. This, therefore, causes less damage and abrasion to the processing equipment. From an economic and an environmental point of view, they are one of the cheapest materials available and they come from renewable and recyclable sources.[3–6] This is fundamental if one takes into account that at present, the annual consumption of wood throughout the world is very high. It is estimated that in the year 2010 the consumption of wood will exceed 4.5 thousand million cubic meter, which means a ratio of 1.5 m^3 per person and per year.[7,8]

Despite these advantages, the use of cellulose-based materials as polyolefin reinforcements has attracted relatively little attention. The possible reasons for this are processing difficulties, their low thermal stability, and their absorption of humidity.[3–5,9,10] Nevertheless, the most important disadvantage is due to their reduced resistance and their low efficiency during the stress transfer, given the incompatibility between hydrophilic polar fibers and hydrophobic apolar polyolefins, which create repulsion forces that lead to poor adhesion or no adhesion at all during blending.

One solution to this problem could be based on the application of physical methods, like a corona treatment or the use of cold plasma, or chemical treatments, like fiber modification using maleic anhydride, organosilanes, isocyanates, sodium hydroxide,

**Present address*: Departamento de Física, E.U.P. Ferrol, Universidad de A Coruña, Avda 19 de Febrero s/n, 15405 Ferrol, Spain.
Correspondence to: L. Barral (labpolim@udc.es).
Contract grant sponsor: Secretaría Xeral de Investigación e Desenrolo, Xunta de Galicia; contract grant number: XUGA-PGIDIT05TMT17201PR.
Contract grant sponsor: European Commission; contract grant number: RII3-CT-2004-506008 (IA-SFS).

permanganate or peroxide,[11–13] benzylation,[14] and acetylation,[15] or through the use of coupling or compatibilizing agents. The purpose of these compatibilizers is to act on the interface, increasing the adhesion between the substrates through the reduction of interfacial tension and then producing finer dispersions and more regular as well as more stable morphologies.[3,11,16–20]

There are coupling agents, such as maleic anhydride, which incorporate OH groups into the matrix with a resulting improvement of the resin moisturization on the fibers. These OH groups later interact with the OH of the lignocellulosic fibers via a hydrogen bond and generate strong fiber–matrix linkages.[19] The SEBS-MA copolymers also exert a compatibilization effect between the various wood-derived fillers and polyolefin matrices. Some authors have shown that various kinds of elastomers are capable of forming an interface around the charged particle and therefore improve the interfacial adhesion among the phases.[4,20–23] SBS has been used as a compatibilizer in low density polyethylene composites, creating a positive effect on mechanical properties and adhesion. However, the effect is relatively weak, since complete coupling between the fiber and the matrix was not successful.[24]

Polypropylene (PP) is a thermoplastic matrix that has received special attention in the production of thermoplastic composites reinforced with natural fibers.[13,15,25–27] The isotactic polypropylene (iPP) composites reinforced with woodflour (WF) have been closely studied over the last few years. Both the influence of water absorption on mechanical properties,[28,29] and the morphology and mechanical properties in the presence or absence of a compatibilizing agent have been analyzed.[23,29–32] Nevertheless, very few studies are related to the analysis of the behavior of the crystallization and the melting of iPP and WF composites.[33,34] Other vegetable fibers, like sisal or bamboo, have already been considered.[34,35]

To venture more deeply into the analysis of the behavior of solid state of isotactic semicrystalline PP in these composite materials, the aim of this work is to study the dynamic crystallization of iPP and its binary composites containing wood derivatives, WF, by means of differential scanning calorimetry. In addition, the composition and the presence of an interface agent used as a compatibilizing system will be considered.

EXPERIMENTAL PROCEDURE

The polypropylene (PP) used was ISPLEN® PP 070 G2M, with a melt flow index of 10.0 g/10 min (230°C/2.16 kg) and a density of 0.902 g cm^{-3} and was provided by Repsol-YPF.

The ionomer used was SURLYN 9970, which corresponds to an ethylene/methacrylic acid copolymer partially neutralized with metallic zinc ions, with a melt flow index of 14.0 g/10 min (230°C/2.16 kg) and a density of 0.940 g cm^{-3} and was provided by Dupont.

The woodflour, WF, was provided by Galparket, S.A. (A Coruña, Spain). It is a oak wood waste made during the manufacture of floors. It was sifted with a metallic sieve with a mesh of 100 μm until a specific distribution of particle size was obtained.

In a stage prior to the preparation of the composites, the WF was kept at 100°C for 24 h in a vacuum oven, while the zinc ionomer was dried at 60°C for 12 h. After the drying stage, the binary composites of polypropylene/woodflour, PP/WF, and the ternary composites of polypropylene/woodflour/ionomer, iPP/ WF/I, were prepared via extrusion. A corotating twin-screw extruder, Brabender DSE 20, was used. It has a constant profile of temperature of 180°C from the feed zone to the die and a screw speed of 45 rpm.

The PP/WF and PP/WF/I blends were kept in a vacuum oven at 80°C for 24 h and 60°C for 24 h, respectively. Later, the test tubes were prepared using injection. A Battenfeld Plus 350 injector was used. It has an injection pressure of 1400 bar, a cylinder temperature of 180°C, and an injection rate of 80 cm^3 s^{-1}. The mold used was made of steel for traction and impact standardized test tubes according to ISO 527.

Binary formulations PP/WF, with 90/10 and 80/20 wt % compositions, and ternary formulations, PP/WF/I, with two different ionomer percentages of 5 and 10 wt % with respect to the WF found in the blend, were studied.

The study of thermal stability of the WF was made in a Mettler TA4000/TG50 thermobalance under an oxygen atmosphere in heating conditions between 50 and 180°C at a heating rate of 10°C min^{-1}. It was followed by a second isotherm stage at 180°C for 120 min with a sample weight between 10 and 12 mg. In this way, the stability of the wood derivative was guaranteed for long intervals of time at the temperature used later during the stage of extrusion and injection molding. The thermal stability analysis of the binary and ternary blends was made in a Perkin–Elmer 7 thermobalance between 50 and 800°C at a rate of 10°C min^{-1}, under an argon atmosphere.

The experiments of differential scanning calorimetry were made in a Mettler TA-4000/DSC30 calorimeter under dynamic conditions. The data was evaluated with a TA 72.2/5 program using aluminum capsules with sample weights of ~12 mg and under an inert nitrogen atmosphere with a volume of 25 mL min^{-1}. The cooling cycles were made from the melt at rates of 20, 10, 4, 2, and 1°C min^{-1}, fol-

lowed by heating cycles at 10°C min^{-1} in an interval of temperatures between 30 and 210°C.

The elimination of the thermal history prior to the crystallization of PP was achieved by retaining the samples at a residence temperature in the melt of 210°C,[36] for 5 min, to eliminate the memory effects and to assure the thermal stability of the WF component to the maximum.

The melt temperature, T_m, and the crystallization temperature, T_c, were determined as the highest temperature of the endotherm melt obtained in the heating scan and the lowest temperature of the exotherm obtained in the cooling process, respectively. The apparent enthalpy of the transition, ΔH_{ap}, was determined as the area below the curve of transformation. The conversion up to crystallinity level $(1 - \lambda)_{DSC}$ was made using the eq. (1), considering the PP composition of each sample and where $\Delta H_{100} = 137.9$ J/g is the enthalpy of 100% crystalline iPP:[37]

$$(1 - \lambda)_{DSC} = 100(\Delta H_{ap}/\%\, iPP\ \Delta H_{100}) \quad (1)$$

The X-ray diffraction experiments with synchrotron radiation were made in HASYLAB, in the DESY Synchrotron in Hamburg. Simultaneous measurements at wide angles, WAXS, and small angles, SAXS, were obtained in real time. They were carried out using a method of angular distribution of dispersed energy, employing a double focus camera composed of a Germanium Ge^{111} monochromator and a series of quartz focusing mirrors. The wavelength corresponding to the (111) plane of Ge^{111} was 1.5 Å. Linear Gabriel WAXS and SAXS detectors were used. The distance between the sample and the detector was 2 m with the entire system under vacuum conditions.

For the calibration of the detector, poly(ethylene terephthalate) in the case of WAXS, and cow cornea in the case of SAXS, were used as standards. A certain angle was assigned to each channel of the detector from the sharp reflections associated with these standards and the edge of the ''beam-stop.'' Film-shaped samples, which were prepared by compression and crystallized, were measured in a Mettler FP90/FP82 HT temperature cell.

In the case of the injected samples, the X-ray diffraction diagrams at wide angles, WAXS, were obtained at room temperature in a Philips diffractometer using Ni-filtered Cu Kα radiation at a scanning rate of 1°C min^{-1} in the angular region 2θ between 5 and 35°.

The relative fraction of the trigonal β-polymorph was determined from the X-ray diffractograms by using the Turner-Jones parameter, k_β, which is given in the following eq. (2):[38]

$$k_\beta = \frac{I_{\beta 1}}{[I_{\beta 1} + (I_{\alpha 1} + I_{\alpha 2} + I_{\alpha 3})]} \quad (2)$$

where $I_{\beta 1}$ is the intensity of the crystalline reflection associated to the plane (300) corresponding to the modification β and $I_{\alpha 1}$, $I_{\alpha 2}$, and $I_{\alpha 3}$ are the intensities of the crystalline reflections associated to the planes (110), (040), and (130) corresponding to the monoclinic polymorph, respectively.[39]

The scanning electron microscopy (SEM) analysis was done in a Jeol JSM-6400 microscopy, using an Oxford Instruments image acquisition and digitalization, on metal-coated fractured samples, metallized Au in a Bal-Tec SCD 004 cathode sputter coater.

RESULTS AND DISCUSSION

To determine the thermal stability of the binary PP/WF composites and the ternary PP/WF/I composites, thermogravimetric analysis was performed on these blends. Although the presence of an interface agent destabilizes the PP/WF blend thermally, the temperature of initial weight loss in an inert nitrogen atmosphere is situated between 240 and 260°C in both systems. This fact is essentially important since it assures the thermal stability of samples during the corresponding crystallization cycles from the melt to the later melting after a residence temperature in the melt of 210°C has been chosen.

In Figure 1, the crystallization exotherms of the original iPP are shown at the cooling rates analyzed. Displacement of the exotherms to regions of lower temperatures and an increase in their width as the cooling rate increases can be observed. This is directly related to the formation of the most imperfect crystals, and therefore, a larger population of crystalline sizes.

The analysis of the crystallization from the melt of the binary PP/WF blends under dynamic conditions reflected the existence of different behaviors depending on composition (Table I).

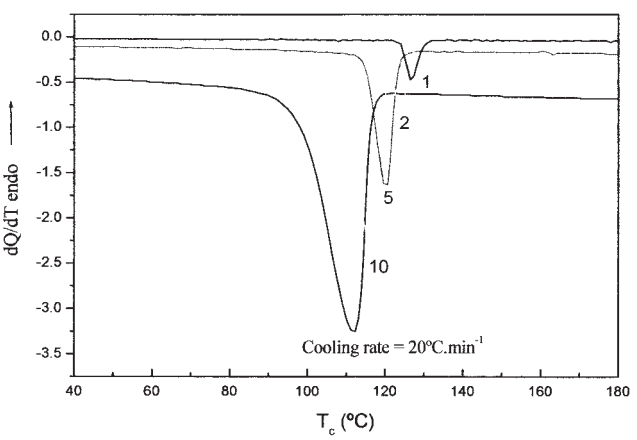

Figure 1 Crystallization exotherms from the melt of PP at the rates specified.

TABLE I
Crystallization Temperatures Obtained for PP/WF/I Blends with Dynamic Crystallization Cycles from the Melt

	T_c (°C) at cooling rates of				
	20°C min^{-1}	10°C min^{-1}	5°C min^{-1}	2°C min^{-1}	1°C min^{-1}
PP	108.5	114.3	118.5	123.0	126.1
90/10	107.4	113.6	117.9	122.5	125.4
90/10/5	103.9	109.2	113.9	118.6	122.3
90/10/10	104.3	109.9	114.3	119.2	122.1
80/20	109.4	115.4	120.1	124.3	127.4
80/20/5	104.7	110.5	114.8	119.7	122.6
80/20/10	105.9	110.1	114.3	118.6	122.1

Although the differences in the values of T_c are very small and could be considered in the interval of calorimetric uncertainty, it is important to point out that in the case of the binary PP/WF 90/10 blend, they are always inferior to those of pure iPP, while in the case of the binary PP/WF 80/20 blend, they are always slightly superior (Figure 2).

In this respect, Albano et al.[34] did not observe variations in the crystallization temperature of the PP/WF 60/40 and PP/sisal fiber 80/20 blends at a cooling rate of 5°C min^{-1}. Xie et al.[40] analyzed the behavior of crystallization and melting of uncompatibilized and injection-molded PP/sisal fiber composites and found increases in the crystallization temperature in the region of 8°C for 10% of fiber. In addition, the authors point out that at the highest fiber concentrations, 20 and 30%, the molecular movement of the PP chains is more restricted and the increase experienced in the crystallization temperature is only 5°C.

Thomason and Van Rooyen[41] studied the isothermal crystallization of PP in the presence of a large variety of fibers using thermo-optic analysis and DSC. They observed that the formation of transcrystallization depends on the nature of fiber and the crystallization temperature. It is known that a transcrystalline layer is formed in the fiber–matrix interface when fibers with enough nucleating capacity are used,[42,43] favoring the stress transfer between the fiber and the matrix.[44] In our case, the observations made by polarized light microscopy on films prepared by compression at the same cooling rates allow us to exclude the existence of transcrystallization phenomena.

The effect caused by the presence of the ionomer used as an interfacial agent on the crystallization temperature of PP is seen in Figures 3 and 4, for 90/10 and 80/20 blends, respectively. The addition of Surlyn 9970 to the binary blends causes a drop in the crystallization temperature. In principle, this is indicative of an increase in compatibility between the iPP and WF components in blends, although it does not seem that the increase of the ionomer concentration, from 5 to 10%, affects the reduction experienced by the T_c (Table I).

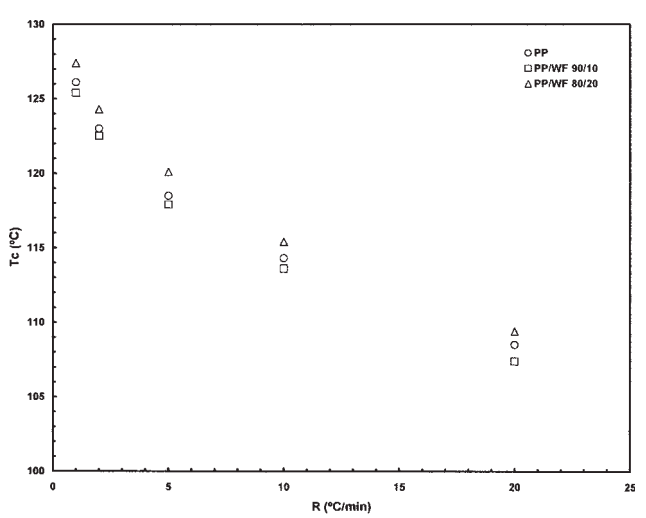

Figure 2 The variation of the crystallization temperature with the cooling rate of the specified blends.

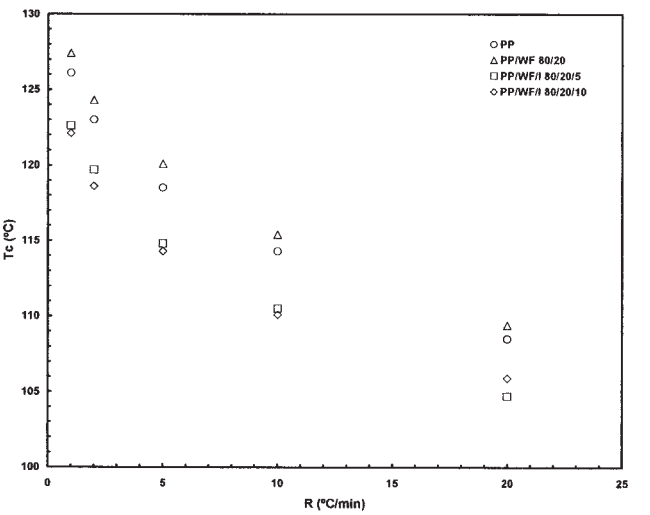

Figure 3 Variation of the crystallization temperature as a function of the cooling rate for the blends specified (80/20 blend).

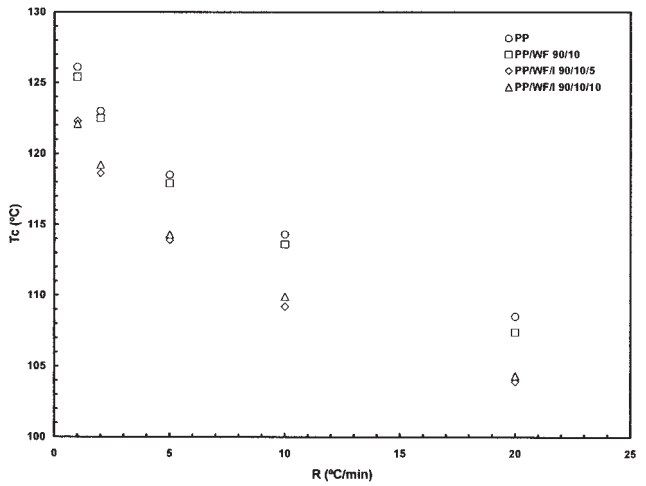

Figure 4 Variation of the crystallization temperature as a function of the cooling rate for the blends specified (90/10 blend).

In the study on the UV ageing of PP/WF composites in the presence of PP-MA as a compatibilizer, Seldén et al.[45] described an increase of $\sim 4^{\circ}C$ in the crystallization temperature of PP for a fiber concentration of 50%. This accounts for the existence of the nucleating effect even in the presence of the interfacial agent.

Núñez et al.[33] analyzed the behavior of PP crystallization in injection-molded PP/WF composites with various compatibility levels by modification with esterification of the WF particles with maleic anhydride, or with the addition of PP-MA to the composites with unmodified WF. They observed that the unmodified PP/WF composites have crystallization temperatures more than 5–10°C higher than that of PP, in a concentration interval between 10 and 40% of WF. The WF composites esterified with MA show an increase in T_c of $\sim 6^{\circ}C$, which seems to be independent of the load concentration between 10 and 50%. In the case of composites with a compatibilizing agent, the increase in the T_c is in the region of 9 and 7°C for a load concentration of 40 and 50%, respectively. The authors concluded that the increase observed in the crystallization temperature in all the composites demonstrates that the nucleating effect induced by the WF particles on the PP matrix is independent of the various compatibility levels.

Mi et al.[46] studied PP crystallization in PP composites with bamboo fiber prepared by compression, using PP matrices with various levels of grafting in MA. They found an increase in the T_c between 1 and 5°C, depending on the level of the grafting in the PP. This is explained by the existence of transcrystallization phenomena around the fibers.

In our case, the variation described in the crystallization temperatures of the ternary blends is not accompanied by very significant changes in the crystalline level developed, which remain between 55 and 60%. Although the differences are minimal, it should be pointed out that the lowest values of crystallinity correspond to the blends that contain 10% ionomer, which is coherent with the increase of compatibility already noted by the drop in the crystallization temperature.

The evolution of the crystallization process from the melt state to the organized state was followed by means of the variation in conversion, or the percentage of crystalline transformation, as a function of temperature for the various cooling rates analyzed. This is detailed in Figure 5 for PP and the binary PP/WF 90/10 blend.

The tendency shown by the conversion curves, with a much accelerated primary crystallization even at the lowest cooling rates, did not allow the application of the Ozawa treatment for the analysis of nonisothermal crystallization kinetics.[47] For this reason,

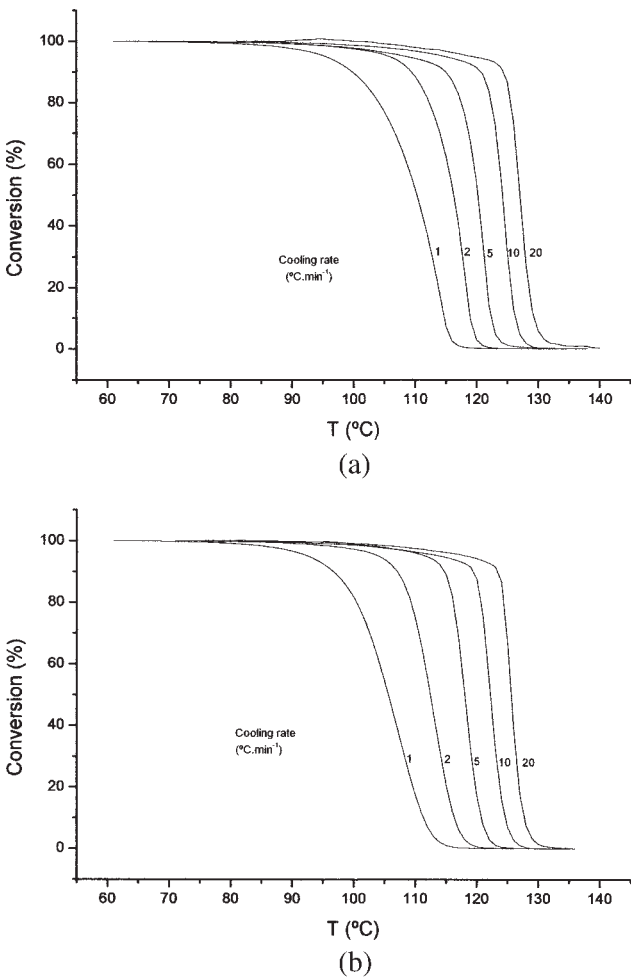

Figure 5 Variation of the conversion with the temperature, during the cooling from the melt for (a) pure PP, and (b) the binary PP/WF 90/10 blends at the cooling rate specified.

TABLE II
T_{10} Values for the Blends as a Function of the Cooling Rate

	T_{10} (°C) values at cooling rates of				
	20°C min^{-1}	10°C min^{-1}	5°C min^{-1}	2°C min^{-1}	1°C min^{-1}
PP	129.5	126.2	122.5	119.0	114.6
90/10	127.8	124.7	120.8	116.4	111.1
90/10/5	125.3	121.3	117.5	112.2	107.2
90/10/10	125.3	121.9	117.8	113.1	108.1
80/20	129.3	125.6	122.5	118.1	112.9
80/20/5	125.6	122.5	118.3	113.6	108.3
80/20/10	125.1	121.2	118.5	112.8	108.2

another kinetic parameter, such as T_{10}, which is defined as the temperature at which 10% of the crystalline transformation is achieved at a predetermined cooling rate (Table II), was used. The choice of this parameter allowed a comparison of the crystallization rate at various cooling conditions for all of the samples analyzed.

A tendency, which is not very significant, can be detected in the drop of the T_{10} value for PP because of the presence of the filler, at all the cooling rates analyzed. It could be interpreted as a small drop in the rate of PP crystallization in the blend. In other words, lower temperatures are necessary to achieve the same level of conversion at the same cooling rate.

On the other hand, using the same criteria of the T_{10} parameter, a marked reduction of the crystallization rate in the ternary blends was observed. In other words, the presence of the ionomer induces the compatibilization of PP and WF acting as an interfacial agent.

This improvement in compatibility corresponds to the information obtained from SEM, after comparing the morphologies associated with binary and ternary blends of the same PP/WF composition. This is shown in Figure 6 for the PP/WF 90/10 and PP/WF/I 90/10/10 samples. In the PP/WF 90/10 blends, cavities and fibrous junctions can be clearly observed in the fracture surface. This indicates that the wood particles were displaced without breaking up. At the same time, the cavities occupied by WF particles show clean surfaces and the fracture levels are very well defined, thus indicating the existence of poor adhesion among the components of binary blend. On the other hand, in the ternary 90/10/10 blend, the surfaces of the WF particles are practically absorbed by the polymeric matrix and it is very difficult to differentiate them. The level of WF dispersion and the interfacial adhesion between the WF and the PP matrix are clearly improved by the presence of the interfacial agent.

Thermograms were obtained in the heating cycle following each previously described dynamic crystallization cycle from the melt. In the case of pure iPP and the binary and ternary blends, one melting endotherm is observed with a maximum situated between 164 and 166°C (Figure 7), and which corresponds to the melting of monoclinic crystals of iPP.

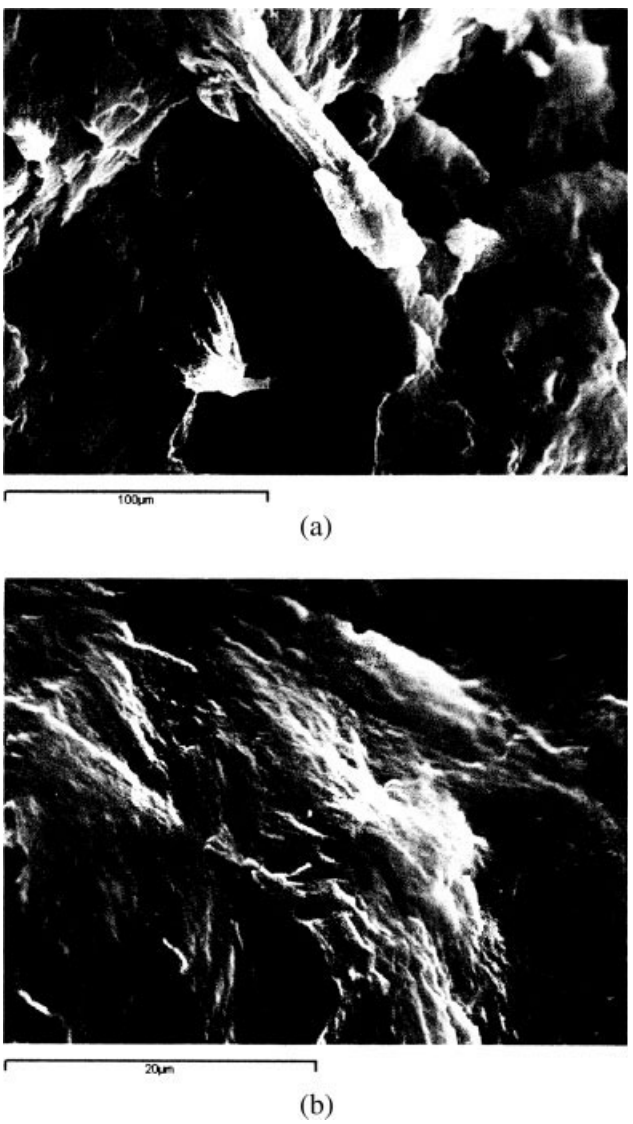

Figure 6 SEM microphotographs of (a) the binary iPP/WF 90/10 composite, and (b) the ternary iPP/WF/I 90/10/10 composite.

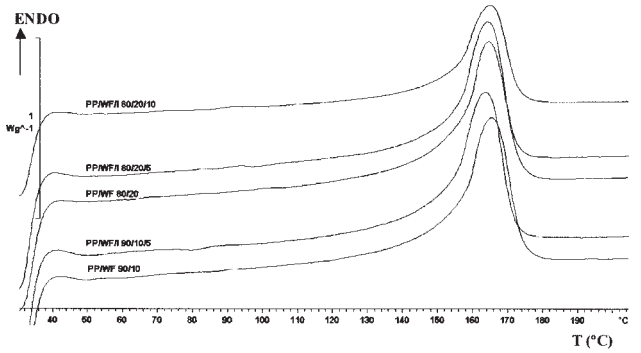

Figure 7 Thermograms of heating, at 10°C min^{-1}, of binary and ternary blends, after crystallization from the melt at a rate of 10°C min^{-1}.

The values of the melt temperature of PP in the ternary blends is slightly inferior to its respective temperature in the binary blends, which is coherent with the existence of compatibilization due to the presence of the ionomer as an interface agent. Albano et al.[34] did not observe any variations in the melt temperature of PP/WF 60/40 blends and PP/sisal fiber 80/20 blends, after the crystallization occurred at a cooling rate of 5°C min^{-1}.

The results obtained agree with the X-ray diffractograms recorded at room temperature, after crystallization at 10°C min^{-1}, for the films of the binary and ternary blends prepared by compression, in which only the main crystalline reflections are shown at $2\theta = 14.2°$, 17.0°, 18.8°, 21.2°, and 22.0°, respectively, for the (110), (040), (130), (111), and (041) planes associated to the α or monoclinic modification of iPP.

Further information on the crystallization (Figure 8) and melting (Figure 9) processes were obtained via real-time X-ray diffraction using synchrotron radiation as a function of temperature. This allowed the confirmation of the absence of other polymorphs different from the monoclinic form in these samples.

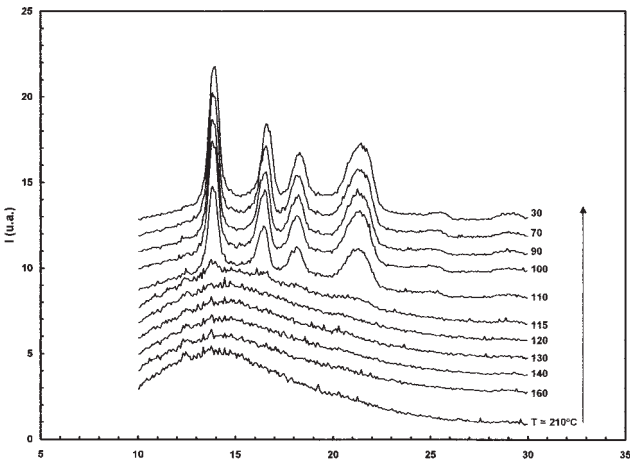

Figure 8 WAXS diffractograms associated with crystallization from the melt of the ternary 90/10/10 blend, at a cooling rate of 10°C min^{-1}.

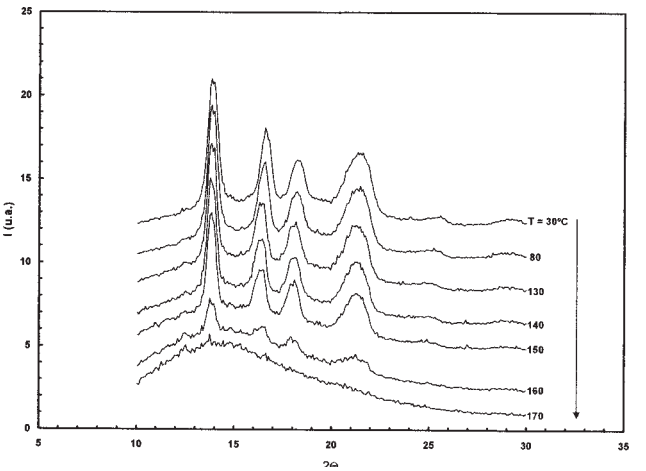

Figure 9 WAXS diffractograms associated with the heating of the ternary 90/10/10 blend, after crystallization from the melt at a cooling rate of 10°C min^{-1}.

On the other hand, when the melting behavior of the blends prepared with injection molding is analyzed (Figure 10), a small shoulder situated in the range between 150 and 155°C is observed, which could correspond to the melting of crystallites of the β-form or trigonal polymorph.[48]

The existence of these type of shoulders or asymmetries found in the lower temperature region of the melting endotherm of iPP can also be associated with the presence of melting–recrystallization–melting processes, which are representative of the imperfection of the crystallites formed during the cooling process from the melt.[49–51]

Nevertheless, analysis of the X-ray diffractograms obtained directly from the test tubes injected at room temperature clearly shows the crystalline reflection at $2\theta = 16.2°$, associated with the plane (300) of trigonal PP, together with those associated with the

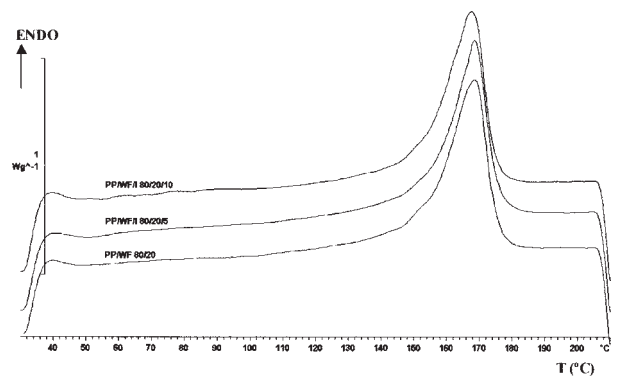

Figure 10 Thermograms of melting, at 10°C min^{-1}, of the injection-molded binary and ternary blends.

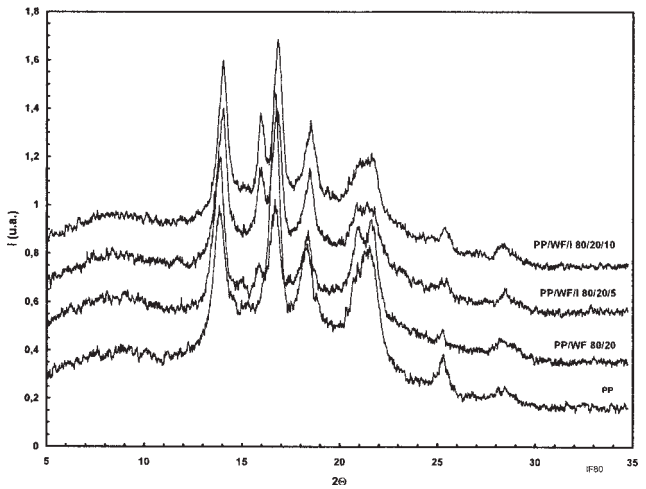

Figure 11 WAXS diffractograms of injected test tubes obtained at room temperatures.

monoclinic iPP polymorph (Figure 11). The values of k_β obtained oscillate very slightly between 0.15 and 0.18 for the binary blends and between 0.22 and 0.25 for ternary samples.

Xie et al.[40] described values for k_β of 0.26, 0.29, and 0.20 in uncompatibilized and injection-molded PP/sisal fiber composites for fiber concentrations of 10, 20, and 30 wt %. However, the addition of a compatibilizing agent, SEBS-MA, to concentrations of 8 and 16 wt % for a composite with 20% sisal fiber reduces the trigonal fraction present in PP up to values of 0.26 and 0.21, respectively. In addition, Son[52] described the formation of a very small percentage of β-form in the PP/cellulose fiber composites, with various fiber treatments, only after undercooling in water of the films prepared by compression.

In the same way, Núñez et al.[33] detected a small endothermic peak at 148°C, corresponding to the trigonal form, during the first heating of injection-molded PP and esterified WF composites with MA. In the case of composites with untreated WF or in which PP-MA was added as a compatibilizing agent, the presence of the β-form was not detected. This β phase was also found by other researchers in PP/bamboo fiber composites[37] and in PP/acetyl jute or grafted with PMMA.[53] As in our case, this small endotherm[33] does not appear in the second heating cycle, after the cooling from the melt, which suggests that the formation of this β microphase takes places during rapid cooling in the injection molding cycle. It has been suggested that the shear flow that occurs in the matrix–fiber interface during the processing of these composites could be important at the time of controlling and modifying the local morphology around the fiber,[53] which becomes more pronounced as the cooling rate increases. On the other hand, these authors[45] confirmed that the presence of the β-form is more evident on the surface of the injection test tubes and weaker in the interior. Moreover, the aforementioned polymorph was not found in similar samples molded by compression, as is our case.

CONCLUSIONS

The analysis of dynamic crystallization by differential scanning calorimetry shows the existence of the different behavior, depending on composition. The crystallization of the PP is affected by the presence of the compatibilizing agent. This presence leads to a reduction in the crystallization temperature, indicative of an increase in compatibility between the iPP and WF. Moreover, in the evolution of the crystallization process a reduction of the crystallization rate in the ternary blends is observed. In other words, the presence of the ionomer induces the compatibilization of the PP and WF components. The morphologies associated with the ternary blends show an improved level of WF dispersion and interfacial adhesion between the components than the binary blends. The results obtained by WAXS confirms the existence of the crystalline reflection associated with the trigonal PP modification.

Therefore, the results obtained from differential scanning calorimetry, X-ray diffraction, and scanning electronic microscope demonstrate the improvement in compatibility of the PP/WF blends. These results seem to confirm the existence of co-operative processes, such as the reduction of the crystallization temperature and the shear effect as a result of the injection molding in the trigonal polymorph generation in the presence of a compatibilizing agent.

The work was performed at the synchrotron facility in Hamburg (Hasylab, DESY) and the authors thank Dr. S. Funari for his technical assistance.

References

1. Shah, N.; Banerjee, N. J Appl Polym Sci 1996, 62, 1199.
2. Amash, A.; Zugenmaier, P. Polymer 2000, 41, 1589.
3. Bledzki, A. K.; Gastan, J. Prog Polym Sci 1999, 24, 221.
4. Bledzki, A. K.; Reihmane, S.; Gastan, J. Polym Plast Technol Eng 1998, 37, 451.
5. Rowell, R. M.; Sanadi, A. R.; Caulfield, D. F.; Jacobson, E. In Lignocellulosic–Plastic Composites; Leao, A. L.; Carvalho, F. X.; Frollini, E., Eds.; USP and UNESP: Sao Paulo, 1997; p 23.
6. Caraschi, J. C.; Leao, L. A. Mater Res 2002, 5, 405.
7. Strykowski, W. Development of Wood-Processing Industry in Poland; Przemysl Drzewny: Poznan, Poland, 1996, 12, 26.
8. Schmincke, K. H. Proc Exp Forestry Res 1996, No. 11.
9. Nuñez, A. J.; Sturn, P. C.; Kenny, J. M. Aranguren, M. I.; Marcivich, N. E.; Reboredo, M. M. J Appl Polym Sci 2003, 88, 1420.
10. Rodríguez, C. A.; Medina, J. A.; Reinecke, H. J Appl Polym Sci 2003, 90, 3466.
11. Ràcz, I.; Hargitai, H. Int J Polym Mater 2000, 47, 667.

12. Joseph, P. V.; Mathew, G.; Joseph, K.; Groenincks, G.; Thomas, S. Compos A 2003, 34, 275.
13. Fung, K. L.; Xing, X. S.; Li, R. K. Y.; Tjong, S. C.; Mai, Y. W. Compos Sci Technol 2003, 63, 1255.
14. Lu, X.; Zhang, M. Q.; Rong, M. Z.; Shi, G.; Yang, G. C. Compos Sci Technol 2003, 63, 177.
15. Albano, C.; González, J.; Ichazo, M.; Kaiser, D. Polym Degrad Stab 1999, 66, 179.
16. George, J.; Sreekala, M. S.; Thomas, S. Polym Eng Sci 2001, 41, 1471.
17. Qingxiu, L.; Matuana, M. L. J Appl Polym Sci 2003, 88, 278.
18. Sun, M. L.; Fena, C. Y.; Yen, W.; Hsun, C. C.; Hsiao, S. F. J Appl Polym Sci 2003, 87, 487.
19. Gauthier, R.; Joly, C.; Compas, A.; Gaultier, H.; Escoubes, M. Polym Compos 1998, 19, 287.
20. Oksman, K. Wood Sci Technol 1996, 30, 197.
21. Long, Y.; Shanks, R. J Appl Polym Sci 1996, 62, 639.
22. Pukanszky, B.; Tudos, F.; Kolarik, J.; Lednicky, F. Polym Composite 1989, 2, 491.
23. Oksman, K.; Clemons, C. J Appl Polym Sci 1998, 67, 1503.
24. Oksman, K.; Lindberg, H.; Holzforschung 1995, 49, 249.
25. Vázquez, A.; Domínguez, V. A.; Kenny, J. M. J Thermoplast Compos Mater 1999, 12, 477.
26. Ichazo, M. N.; Albano, C.; González, J.; Perera, R.; Candal, M. V. Compos Struct 2001, 54, 207.
27. Fung, K. L.; Li, R. K. Y.; Tjong, S. C. J Appl Polym Sci 2002, 85, 169.
28. Stark, N. J Thermoplast Compos Mater 2001, 14, 421.
29. Douglas, P.; Murphy, W. R.; McNally, G.; Billham, M. SPE ANTEC 2003, 2029.
30. Miguez Suárez, J. C.; Coutinho, F. M. B.; Sydenstricker, T. H. Polym Test 2003, 22, 819.
31. Arribas, J. M.; Gómez, J. J.; Perea, J. M.; Marco, C. Rev Plást Mod 2004, 88, 554.
32. Sombatsompop, N.; Yotinwattanakumtorn, C.; Thongpin, C. J Appl Polym Sci 2005, 97, 475.
33. Núñez, A. J.; Kenny, J. M.; Reboredo, M. M.; Aranguren, M. I.; Marcovich, N. E. Polym Eng Sci 2002, 42 733.
34. Albano, C.; Reyes, J.; Ichazo, M. González, J. Brito, M.; Moronta, D. Polym Degrad Stab 2002, 76, 191.
35. Xie, X. L.; Li, R. K. Y.; Tjong, S. C.; Mai, Y. W. Polym Compos 2002, 23, 319.
36. Marco, C.; Ellis, G.; Gómez, M. A.; Arribas, J. M. J Appl Polym Sci 2002, 84, 2440.
37. Fatou, G. Eur Polym J 1971, 7, 1057.
38. Turner-Jones, A.; Aizlewood, J. M.; Beckett, D. R. Makromol Chem 1964, 75, 134.
39. Karger-Kocsis, J., Ed. Polypropylene: Structure, Blends and Composites Vol. 1; Chapman and Hall: New York, 1995.
40. Xie, X. L.; Fung, K. L.; Li, R. K. Y.; Tjong, S. C.; Mai, Y. W. J Polym Sci Part B: Polym Phys 2002, 40, 1214.
41. Thomason, J. L.; Van Rooyen, A. A. J Mater Sci 1992, 27, 889.
42. Wang, C.; Wang, L. M. J Polym Sci Part B: Polym Phys 1996, 34, 1435.
43. Wang, C.; Liu, C. R. Polymer 1997, 38, 4715.
44. Félix, J. M.; Gatenholm, P. J Mater Sci 1994, 29, 3043.
45. Seldén, R.; Nyström, B.; Längstrom, R. Polym Compos 2004, 25, 543.
46. Mi, Y.; Chen, X.; Guo, Q. J Appl Polym Sci 1997, 64, 1267.
47. Ozawa, T. Polymer 1971, 12, 150.
48. Marco, C.; Gómez, M. A.; Ellis, G.; Arribas, J. M. J Appl Polym Sci 2002, 86, 531.
49. Bogoeva, G.; Janevski, A.; Grozdanov, A. J Appl Polym Sci 1998, 67, 395.
50. Paukheri, R.; Lethinen, A. Polymer 1993, 34, 4075.
51. Paukheri, R.; Lethinen, A. Polymer 1993, 34, 4083.
52. Son, S. J. J Mater Sci 2000, 35, 5767.
53. Bhattacharya, S. K.; Shembekar, V. R. Macromol Rep A 1995, 32, 485.
54. Folkes, M. J. In Polypropylene: Structure, Blends and Composites, Vol. 3; Karger-Kocsis, J., Ed.; Chapman and Hall: London, 1995.